Article

Catalytic Alkane Transfer Dehydrogenation by PSP-pincer-ligated Ruthenium. Deactivation of An Extremely Reactive Fragment by Formation of Allyl Hydride Complexes

Xiaoguang Zhou, Santanu Malakar, Tian Zhou, sathiyamoorthy Murugesan, Carlos Huang, Thomas J Emge, Karsten Krogh-Jespersen, and Alan S. Goldman

ACS Catal., **Just Accepted Manuscript** • Publication Date (Web): 26 Mar 2019

Catalytic Alkane Transfer Dehydrogenation by PSP-pincer-ligated Ruthenium. Deactivation of An Extremely Reactive Fragment by Formation of Allyl Hydride Complexes

Xiaoguang Zhou, Santanu Malakar, Tian Zhou, Sathiyamoorthy Murugesan, Carlos Huang, Thomas J. Emge, Karsten Krogh-Jespersen, and Alan S. Goldman*

Department of Chemistry and Chemical Biology, Rutgers, The State University of New Jersey, New Brunswick, New Jersey 08903, United States

ABSTRACT: Iridium complexes bearing PCP-type pincer-ligands are the most effective catalysts reported to date for the low-temperature (≤ ca. 200 °C) dehydrogenation of alkanes. To investigate the activity of formally isoelectronic ruthenium complexes we have synthesized the neutral 2,7-di-*tert*-butyl-4,5-bis(diisopropylphosphino)-9,9-dimethylthioxanthene (^{iPr}xanPSP) pincer ligand and several Ru complexes thereof. The (^{iPr}xanPSP)Ru complexes catalyze alkane transfer dehydrogenation of the benchmark cyclooctane/*t*-butylethylene (COA/TBE) couple with turnover frequencies up to ca. 1 s^{-1} at 150 °C and 0.2 s^{-1} at 120 °C, the highest rates for alkane dehydrogenation ever reported at such temperatures. Dehydrogenation of *n*-octane, however, is much less effective. A combination of experiment and DFT calculations allow us to explain why (^{iPr}xanPSP)Ru is more effective than (^{iPr}PCP)Ir for dehydrogenation of COA while the reverse is true for dehydrogenation of *n*-alkanes. Considering only in-cycle species and simple olefin complexes, the (^{iPr}xanPSP)Ru fragment is calculated to be much more active than (^{iPr}PCP)Ir for dehydrogenation of both COA and *n*-alkanes. However, the resting state in the (^{iPr}xanPSP)Ru-catalyzed transfer dehydrogenation of *n*-alkane is a very stable linear-allyl hydride complex, whereas the corresponding cyclooctenyl hydride is much less stable.

KEYWORDS: Alkane dehydrogenation, pincer ligand, ruthenium, catalyst deactivation, allyl complexes

■ INTRODUCTION

Complexes of pincer ligands have been studied extensively over the past two decades owing to the unique ability which they offer to tune steric and electronic properties, and to a tendency to form highly robust complexes. Pincer complexes are reported in the literature with motifs (named according to the coordinating atoms) that include NCN[1], NNN[2-4], PNP[5-11], PNN[3], SCS [12-13], SNS[14], CNC[15] and PCP[16-19]. They have been widely used for numerous organic transformations, including, *inter alia*, cross-coupling reactions, reduction of carbon dioxide, hydrogenations of polar substrates, hydrosilylation reactions, dehydrogenation of alcohols, and hydroaminations[3-8, 17-38].

Among the most widely investigated classes of pincer complexes have been those with the PCP motif with a central aromatic group and phosphine donor groups at the terminal positions. (PCP)Ir complexes (including bis-phosphinite POCOP complexes, their PSCOP derivatives, and many others) occupy an apparently privileged position in the area of catalytic alkane dehydrogenation.[39-40] We have investigated several isoelectronic analogues of (PCP)Ir complexes for alkane dehydrogenation activity, including Rh^{I} and Os^{0} congeners[7, 10, 41] as well as non-PCP Ir^{I} complexes.[42-43] In some cases these complexes have shown catalytic activity, but not at a level comparable to the (PCP)Ir complexes. Interestingly, perhaps the most active alternatives to (PCP)Ir-catalysts to date have been based on (PCP)Ru fragments[16, 44] although the neutral (PCP)Ru unit is not isoelectronic with (PCP)Ir. Accordingly, such complexes are thought not to proceed via a mechanism that is fully analogous to that of (PCP)Ir complexes.[16]

(PNP)Ru is the ruthenium-based fragment most closely related to (PCP)Ir (Scheme 1). However, although extensive studies by Milstein and others have revealed an extraordinary

range of important catalytic activity by (PNP)Ru species, they have not been reported effective for alkane dehydrogenation.[4, 9, 37, 45-46] In the context of other pincer-ruthenium fragments that are isoelectronic with (PCP)Ir, we considered (PSP)Ru in part because we thought the PSP ligand would bind strongly enough to allow its use at the relatively high temperatures typically required for alkane dehydrogenation.

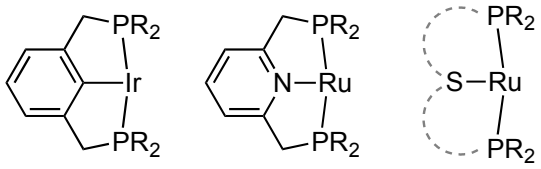

Scheme 1. Isoelectronic Fragments (PCP)Ir and (PNP)Ru, and Motif of a Generic (PSP)Ru Fragment

Although sulfur ligands and thioethers are of course well known to bind well to metal centers,[47-48] and generally more strongly than their oxygen congeners, the chemistry of PSP complexes has been less well developed than that of the analogous POP complexes.[41, 49-50] However, complexes of Ru[51-54], Pt [55-56], Pd [57-58], Rh [59-60], Cr[61], Tc[62] and Re[62], bearing a PSP tridentate ligand have been reported. PSP pincer ruthenium complexes in particular have seen application in alcohol/ketone transfer hydrogenation[51], olefin cyclopropanation[52], and catalytic dehydrogenation of dimethylaminoborane to release H_2.[54]

■ RESULTS AND DISCUSSION

1. Synthesis of (^{iPr}xanPSP)Ru Complexes. Following the synthesis of ^{Ph}xanPSP by Emslie *et al.*[56] (^{R}xanPSP = 2,7-di-*tert*-butyl-4,5-bis(PR_2)-9,9-dimethylthioxanthene), we synthesized ^{iPr}xanPSP and ^{tBu}xanPSP. Addition of two equiv ^{iPr}xanPSP to [*p*-cymene$RuCl_2$]$_2$ in toluene gave

diamagnetic complexes with spectroscopic features consistent with products of displacement of *p*-cymene by ^{iPr}xanPSP (Scheme 2); we tentatively assign these complexes as a mixture of di- and tri-chloro bridged dimers, $[(^{iPr}xanPSP)RuCl_2]_2$ and $[(^{iPr}xanPSP)_2Ru_2Cl_3][Cl]$.[54, 63] Addition of THF led to an equilibrium between these species and a monomeric THF adduct.[64]

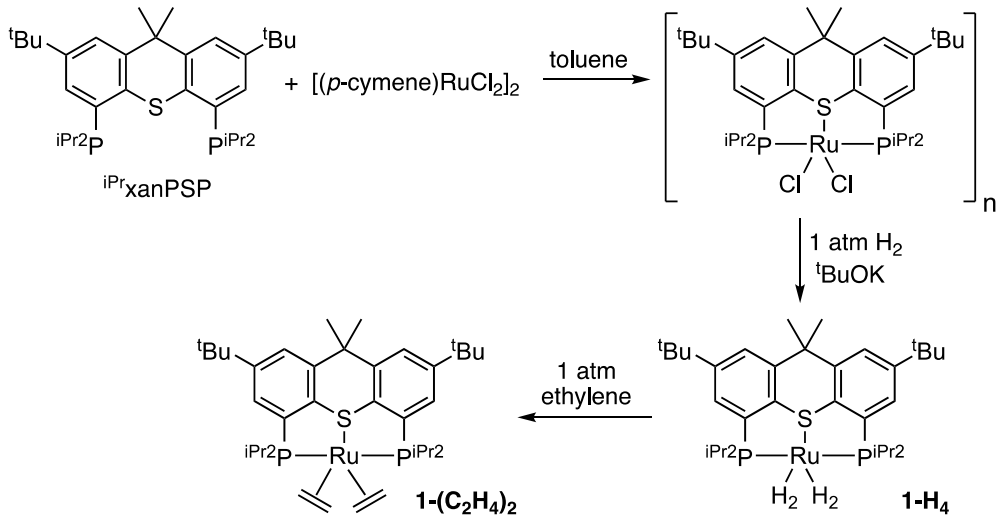

Scheme 2. Synthesis of 1-$(C_2H_4)_2$

In toluene, $[(^{iPr}xanPSP)RuCl_2]_n$ reacts with H_2 to yield a complex which we assign, based on ^{31}P and ^1H NMR spectroscopy,[64] as $(^{iPr}xanPSP)RuCl_2H_2$; a signal at δ -12.50 (2H) may be attributed to two terminal hydrides or a dihydrogen ligand. Treatment of this complex with *t*-BuOK under H_2 atmosphere yields a new complex with one broad singlet hydride peak (δ -8.2, 4H) in the ^1H NMR spectrum at room temperature, which resolves to two broad singlets at -45 °C (Figure S39). The T_1(min) of the two hydride peaks (24.5 ms and 28.6 ms) indicates that this species is a bis(dihydrogen) complex, **1-H_4** (Scheme 2). **1-H_4** is unstable at room temperature in the absence of H_2 atmosphere; the color of a toluene solution slowly turns dark from pale yellow in several hours. The ^1H NMR spectrum showed that H/D exchange with toluene-d_8 solvent also occurred

at room temperature over the course of several hours, with loss of the hydride signal relative to the ^{iPr}xanPSP ligand resonances.

When a toluene solution of **1-H$_4$** was charged with 1 atm ethylene, ^{31}P and ^{1}H NMR spectra revealed a product consistent with formulation as (^{iPr}xanPSP)Ru(C_2H_4)$_2$, **1-(C_2H_4)$_2$** (Scheme 2). This assignment was confirmed by single-crystal X-ray diffraction (Figure 1). The molecular structure of **1-(C_2H_4)$_2$** shows the Ru, P and S atoms to be very nearly in the same plane (with Ru only 0.16 Å out of the P-S-P plane), as with a typical pincer complex geometry. However, in contrast to typical pincer complexes, the overall geometry has neither an approximate mirror plane containing the pincer ligand, nor even approximate C_2 symmetry. Instead the pincer ligand has adopted a pronounced bowl-like structure. This is in contrast with complexes of the ether analogue ^{iPr}xanPOP, in which the ligand adopts a planar or approximately planar configuration when coordinated in a tridentate meridional (i.e. pincer) fashion[41, 65-66]. The difference is presumably attributable to the greater tendency of O than S toward sp^2 hybridization as well as the greater length of the Ru-S bond compared with a Ru-O bond. The pyramidal geometry at sulfur **1-(C_2H_4)$_2$** (the average of the bond angles formed by the three bonds to S is 103.9°) allows the approximately meridional coordination geometry at ruthenium. As a result of this severe distortion from overall planarity of the PSP ligand the ethylene ligands are inequivalent and there are four peaks in the ^{1}H NMR spectrum attributable to coordinated ethylene.

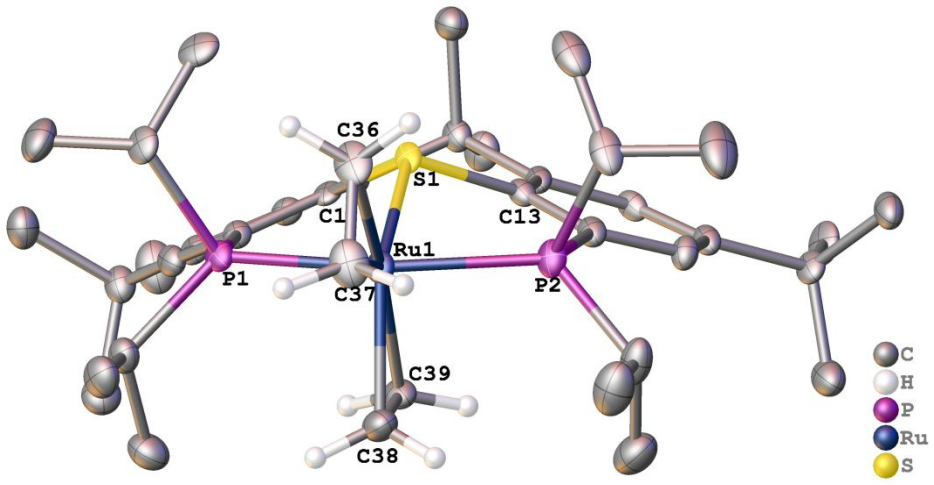

Figure 1. Molecular structure of **1-(C_2H_4)$_2$** determined by single crystal XRD. H atoms other than those on ethylene ligands omitted for clarity. Thermal ellipsoids shown at 50% probability level. Selected distances (Å) and angles (°): Ru1-S1 2.314(1), Ru1-P1 2.354(1), Ru1-P2 2.336(1), Ru1-C36 2.203(5), Ru1-C37 2.156(5), Ru1-C38 2.148(5), Ru1-C39 2.189(5), C36-C37 1.435(7), C38-C39 1.422(7), P1-Ru1-P1 161.02(5), S1-Ru1-P1 80.86(4), S1-Ru1-P2 81.31(4), C39-Ru1-S1 91.7(1), C36-Ru1-S1 100.7(1), C(13)-S(1)-C(1) 99.5(2), C(13)-S(1)-Ru(1) 106.1(2), C(1)-S(1)-Ru(1) 106.11(2)

A one-pot synthesis of **1-(C_2H_4)$_2$** (Scheme 2) in which ^{iPr}xanPSP and [(*p*-cymene)$RuCl_2$]$_2$ were allowed to react in toluene, followed by addition of H_2/*t*-BuOK and then ethylene, afforded a 50% yield of **1-(C_2H_4)$_2$**. Synthesis of the ^{tBu}xanPSP analogue was also attempted, but the initial metalation step appeared to be unsuccessful.

2. Catalytic Alkane Dehydrogenation. 1-(C_2H_4)$_2$ was first investigated as a pre-catalyst for alkane transfer-dehydrogenation with the benchmark acceptor/alkane couple,[39-40] TBE (300 mM) in COA solvent (7.43 M) ([**1-(C_2H_4)$_2$**] = 1.0 mM) (Scheme 3). Remarkably, at 180 °C, transfer-dehydrogenation was complete in 5 min, which corresponds to an average turnover frequency of 1.0 s^{-1} (Figure 2a). The maximum TOF is presumably much greater since this average includes time required to approach 180 °C and time after the reaction was over. Even at 150 °C the reaction was nearly complete after 5 min (230 TO; average TOF = 0.8 s^{-1}), reaching completion

within 60 min (Figure 2c). At 120 °C, the reaction was more than 50% complete after 30 min (average TOF = 0.1 s^{-1}) and was complete within 250 min (Figure 2e). When a drop of mercury was added to the reaction mixture the activity was unchanged, indicating that the reaction does not proceed via colloidal metal.[67] To our knowledge these values represent the fastest reported examples of alkane transfer-dehydrogenation by any solution-phase (or supported molecular) catalyst, or indeed any catalyst, at these relatively low temperatures.[68-72] For example, to our knowledge the fastest previous example at 150 °C was reported by Huang and co-workers; (NCP)IrHCl (NCP = 2-((di-*tert*-butylphosphaneyl)oxy)-6-(pyridin-2-yl)phenyl) catalyzed COA/TBE hydrogen transfer with 168 TO obtained after 10 min (average TOF = 0.28 s^{-1}).[72] We are not aware of reports of any comparable catalyses effected at or near 120 °C.

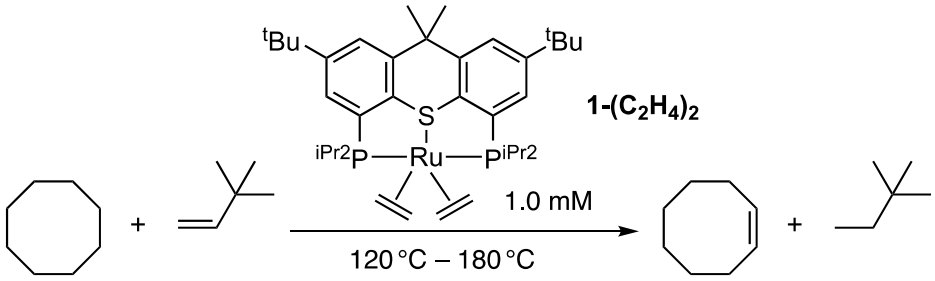

Scheme 3. COA/TBE Transfer Dehydrogenation Catalyzed by (^{iPr}xanPSP)Ru

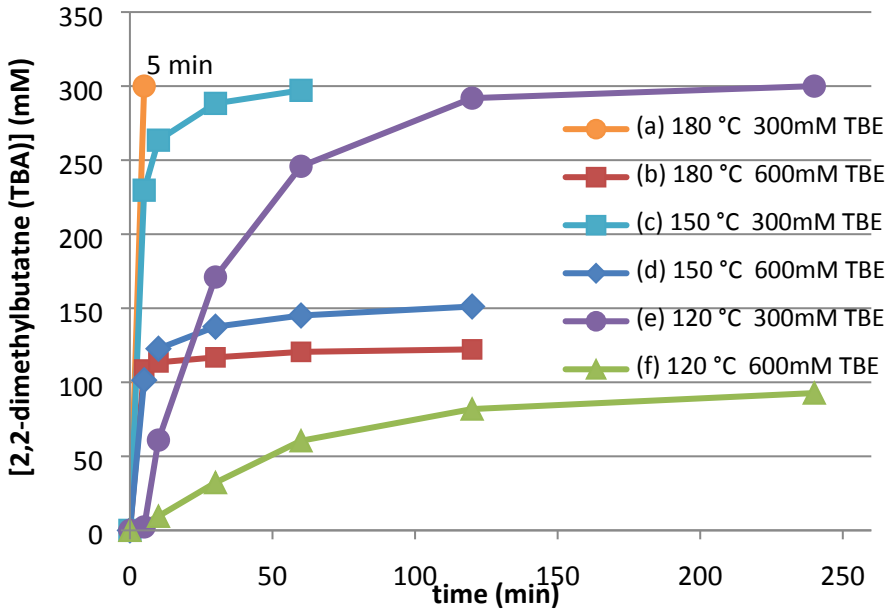

Figure 2. COA/TBE transfer dehydrogenation catalyzed by **1-$(C_2H_4)_2$** (1.0 mM in cyclooctane solvent) at 120 °C, 150 °C, and 180 °C with 300 mM TBE and 600 mM TBE.

A short induction period was noted at 120 °C (Figure 2e). After 5 min only 2.3 TO had resulted whereas (in a separate run) 61 TO were obtained after 10 min (indicating an average TOF of 0.2 s^{-1} after the first 5 min), and 171 TO after 30 min. We attribute the induction period to the time required for the **1-$(C_2H_4)_2$** precursor to lose ethylene. Note that although ethylene is expected to bind much more strongly than TBE to **1**, thereby inhibiting the reaction, it is also presumably much more readily hydrogenated[69]; therefore, once the reaction gets underway and hydride is formed, the ethylene is expected to be quickly removed from the system.

With a higher concentration of TBE, 600 mM, initial rates were somewhat slower, perhaps due to inhibition by coordination of TBE (Figure 2b, d, f). But a much more dramatic difference was that the reaction never approached completion or even approached the product concentration of 300 mM that was obtained with 300 mM TBE. The very different reaction

profile with 600 mM vs. 300 mM TBE strongly indicates an effect of impurities in the commercially obtained TBE. In particular, Roddick has reported that isoprene impurity in TBE can act as a catalyst poison[73] (and presumably precursors of isoprene, or perhaps other small olefins or precursors thereof, could do the same). Accordingly, when a lower grade of TBE (97%) was used the activity was dramatically decreased. We therefore distilled TBE (higher-grade; 98.5%) to obtain a lower-boiling-point fraction and a residue. In accord with the proposed effect of isoprene (b.p. 34 °C) (or perhaps other light olefins or olefin-precursors), the turnover rates and numbers obtained using the distillate were significantly lower than those obtained with the undistilled TBE, while activity obtained with the residue was greater than with undistilled TBE (Figure 3).

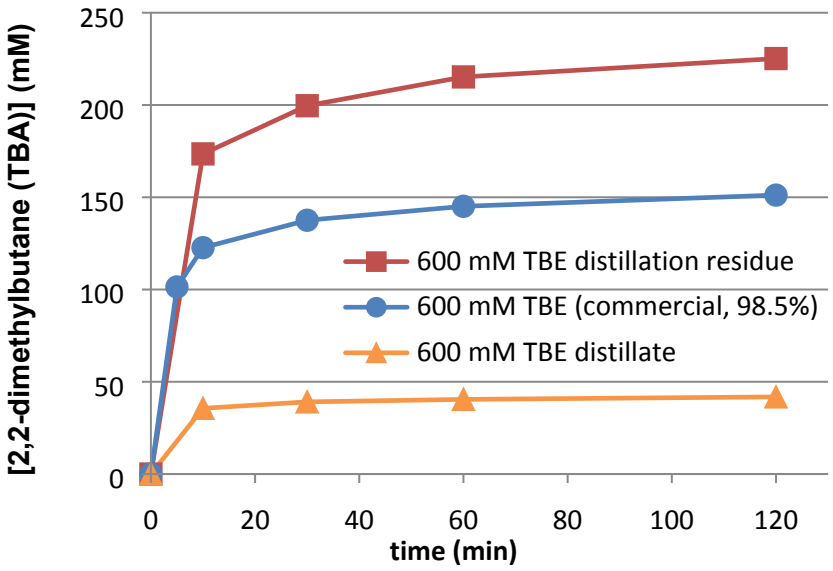

Figure 3. COA/TBE (600 mM) transfer dehydrogenation catalyzed by **1-$(C_2H_4)_2$** (1.0 mM in cyclooctane solvent) at 150 °C, with commercially obtained TBE (98.5%), and with the distillate and residue from its distillation.

While the level of catalytic activity with the benchmark COA/TBE couple was found to be extremely high, results with *n*-octane were significantly less favorable. For example, as noted

above, after 5 min at 150 °C with 300 mM TBE and 1 mM precatalyst in COA solvent, 230 TO were obtained (Figure 4a). In contrast, with *n*-octane, after 120 min only 17 TO were obtained and only 32 TO after 2400 min under the same conditions (Figure 4d).

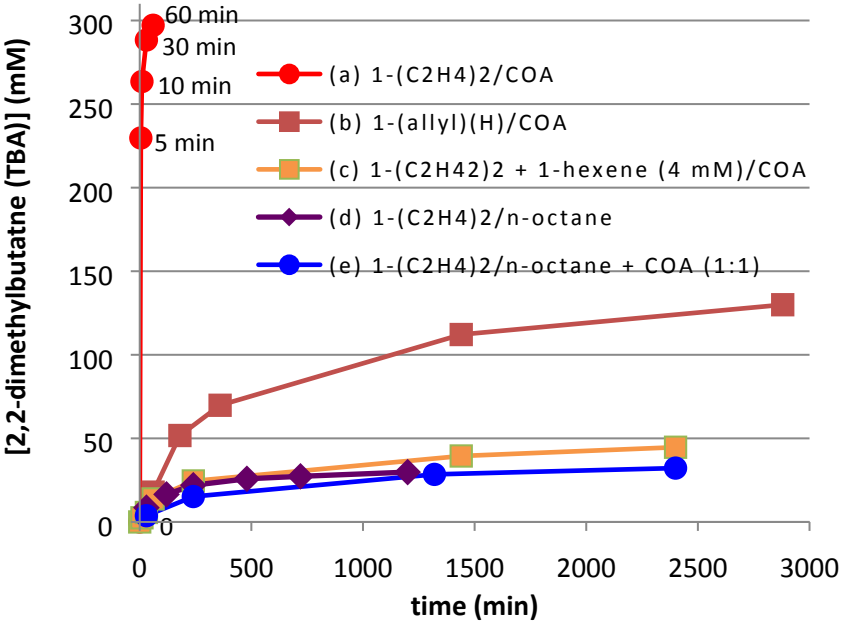

Figure 4. Alkane transfer dehydrogenation ([TBE] = 300 mM) catalyzed by (^{iPr}xanPSP)Ru precursors (1.0 mM) at 150 °C. (a) **1-$(C_2H_4)_2$** in COA (b) **1-(η^3-allyl)(H)** in COA (c) **1-$(C_2H_4)_2$** in COA with 1-hexene (4.0 mM) added (d) **1-$(C_2H_4)_2$** in *n*-octane (e) **1-$(C_2H_4)_2$** in *n*-octane/COA (1:1 v:v).

The much lower TOF and TONs obtained with *n*-octane would seem to suggest that it is a much less reactive substrate. This might seem unsurprising since the dehydrogenation enthalpy of COA (ca. 23 kcal/mol) is much less than that of *n*-octane (28 kcal/mol at C2-C3 and 30 kcal/mol at the terminal position).[74-75] However, we have found that (^{tBu}PCP)Ir is actually selective for dehydrogenation of *n*-alkanes over COA in competition experiments, but inhibition by linear olefin products results in slightly lower rates of *n*-alkane dehydrogenation in independent experiments.[76]

In the context of the above, we prepared a COA solution 1.0 mM **1-$(C_2H_4)_2$** and 300 mM TBE to which was added 1-hexene (to 4.0 mM). Dehydrogenation activity was reduced dramatically by even this low concentration of 1-alkene (Figures 4a and 4c). With COA and *n*-octane (1:1 v:v) the dehydrogenation activity was even lower (Figure 4e), presumably due to the formation of linear octenes although COE was the only olefin that was detected.

We also note that despite (^{iPr}xanPSP)Ru being an excellent catalyst for transfer dehydrogenation of COA, it is found not to be very effective for *acceptorless* dehydrogenation of the same substrate. For example, upon heating a COA solution of **1-$(C_2H_4)_2$** (1.0 mM) to reflux (151 °C) in an argon-purged vessel, 3.6 mM COE was observed after 30 min (of which 2.0 mM was likely due to hydrogenation of the initially coordinated C_2H_4), with total concentrations of 4.5 mM COE and 14 mM COE obtained after 1.0 h and 48 h respectively. This contrasts with previously reported results for acceptorless dehydrogenation of COA by (^{iPr}PCP)IrH_2 (1.0 mM) which yielded 47 mM COE after 30 min and 105 mM after 15 h.[77]

3. Speciation: Formation of Allyl Complexes. The reactions of **1-$(C_2H_4)_2$** with 1-hexene, propene or β-methylstyrene at 70 °C to 100 °C in toluene-d_8 all led to compounds that showed an AB pattern in the ^{31}P NMR spectrum with resonances at ca. δ 86 and δ 90 (1-hexene, 86.4, 89.4 ; propene, 87.3, 92.8; 2-methylstyrene, 85.6, 88.5) and J_{PP} = 263 – 265 Hz (Scheme 4). The ^{1}H NMR spectra of the PSP ligands are likewise consistent with an absence of molecular symmetry; for example two inequivalent backbone *t*-Bu groups are clearly observed. A peak at ca. δ -11 in the ^{1}H NMR spectra is a doublet of doublets ($^2J_{PH}$ = 30.8 Hz, 22.1 Hz for the product of the propene reaction) indicative of a hydride coupled to two inequivalent phosphino groups. All spectroscopic data are consistent with the assignment of these species as (^{iPr}xanPSP)Ru(η^3-

allyl)(H) (**1-(η^3-allyl)(H)**), and derivatives thereof, with the allyl ligand oriented so that the phosphino groups are inequivalent. The chemical shifts of the allyl group C2 protons are quite downfield (1-hexene, δ 4.85-4.95; propene, δ 5.07; β-methylstyrene, δ 5.87) while the C1 and C3 protons resonate at ca. δ 1.0 to δ 2.5, in agreement with reported Ru^{II} allyl and phenylallyl complexes.[78] Confirming the assignment, we obtained crystals from the reaction with propene which allowed X-ray crystallographic determination of the structure (Figure 5).

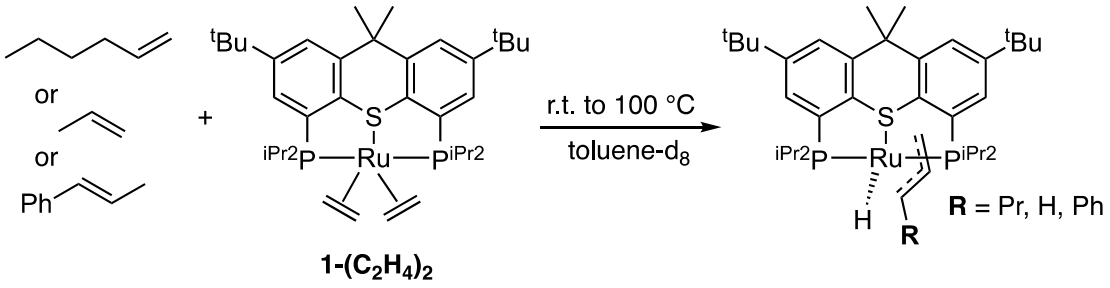

Scheme 4. Formation of Allyl Complexes from 1-(C_2H_4)$_2$

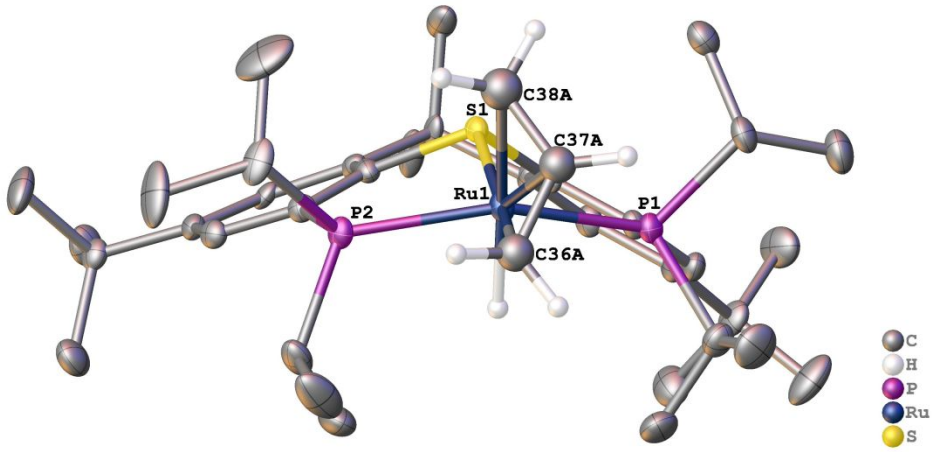

Figure 5. Molecular structure of **1-(η^3-allyl)(H)**, obtained from the reaction of **1-(C_2H_4)$_2$** with propene, determined by single crystal XRD. H atoms (except allyl group and hydride) omitted for clarity. Thermal ellipsoids shown at 50% probability level. Selected distances (Å) and angles (°): Ru1-S1 2.2652(10), Ru1-P1 2.2995(11), Ru1-P2 2.3081(10), Ru1-C36A 2.227(5), Ru1-C37A 2.185(5), Ru1-C38A 2.239(5), S(1)-Ru(1)-P(1) 82.83(3), S(1)-Ru(1)-P(2) 84.26(3), C(36A)-Ru(1)-S(1)

167.0(2), C(38A)-Ru(1)-S(1) 102.7(2), C(36A)-Ru(1)-P(1) 104.6(3), C(36A)-Ru(1)-P(2) 93.4(3), C(37A)-Ru(1)-P(1) 92.87(19), C(37A)-Ru(1)-P(2) 114.8(2), C(38A)-Ru(1)-P(1) 110.9(3), C(38A)-Ru(1)-P(2) 97.4(3)

1-(η^3-allyl)(H) (1 mM) was found to act as a catalyst precursor for COA/TBE dehydrogenation (Figure 4b), but was far less active than **1-$(C_2H_4)_2$** (Figure 4a). The activity of this solution was, however, much greater than that obtained from a COA solution of **1-$(C_2H_4)_2$** to which 1-hexene (4.0 mM) had been added (Figure 4c).

A *p*-xylene-d_{10} solution of *n*-octane (500 mM), **1-$(C_2H_4)_2$** (10 mM), and TBE (500 mM) was heated to 150 °C and monitored by ^{1}H and ^{31}P NMR. The resulting NMR spectra were essentially identical to those resulting from the reaction with 1-hexene; presumably this is attributable to the η^3-octenyl analogue of the η^3-hexenyl hydride complex. The observation of this species as the resting state during octane dehydrogenation (Figure S43), and the observation that addition of 1-hexene or *n*-octane to a COA solution strongly inhibits COA dehydrogenation (Figure 4c, e), indicate that the stability of these allyl hydrides accounts at least in large part for the relatively low level of activity for *n*-alkane dehydrogenation.

After heating a COA solution of **1-$(C_2H_4)_2$** (28 mM) and TBE (780 mM) for 9 min at 130 °C, an AB pattern similar to those of the linear allyl hydrides was observed in the ^{31}P NMR spectrum, with chemical shifts of δ 79.8 and δ 92.8 and J_{PP} = 253 Hz. In the ^{1}H NMR spectrum a hydride peak (dd) was present at δ -11.35 with P-H coupling constants of 36.6 Hz and 22.8 Hz, similar to the hydride of the linear allyl hydride complexes. In analogy with the linear allyl hydrides, we assign this species as a cyclo-η^3-allyl hydride. In addition, a singlet at δ 84.0 was observed in the ^{31}P NMR spectrum, representing a species present at concentration comparable to that of the putative cyclo-η^3-allyl hydride. In accord with this assignment, the reaction of **1-$(C_2H_4)_2$** with

cyclooctene (COE) in benzene or toluene at 100 °C for 4 h afforded the same set of resonances in the ^{31}P NMR spectrum (Figure S44). Therefore it appears that COE, like linear olefins, reacts with the (^{iPr}xanPSP)Ru fragment to afford an η^3-allyl hydride, but also the species with chemical shift δ 84.0 which we propose to be the simple η^2-cyclooctene adduct.

To independently obtain the proposed cyclo-η^3-allyl hydride, we added 1,3-COD (3 equiv) to **1-H$_4$**. This indeed yielded, as determined by ^{1}H NMR, ^{13}C NMR, gCOSY, gHSQC and ^{31}P NMR spectroscopies, the pure complex that was proposed to be the cyclo-η^3-allyl hydride. The ^{13}C NMR spectrum, in addition to the aromatic peaks, showed two singlets in the far downfield region (δ 141.00, δ 119.01) which by gHSQC were correlated to the vinyl peaks in the ^{1}H NMR spectrum (δ 6.90, δ 5.35-5.46). In addition to the three allylic peaks (δ 81.41, δ 55.98, δ 42.94), only three signals attributable to secondary carbons were present in the ^{13}C NMR spectrum. The gCOSY and large chemical shift difference in the ^{1}H NMR and ^{13}C NMR signals indicate that vinyl carbons are adjacent to the allyl group. These spectroscopic features are all consistent with characterization as a 3,4,5-η^3-octa-1,2-dienyl complex, (^{iPr}xanPSP)Ru(3,4,5-η^3-octa-1,2-dienyl)(H)[79-80] (Scheme 5).

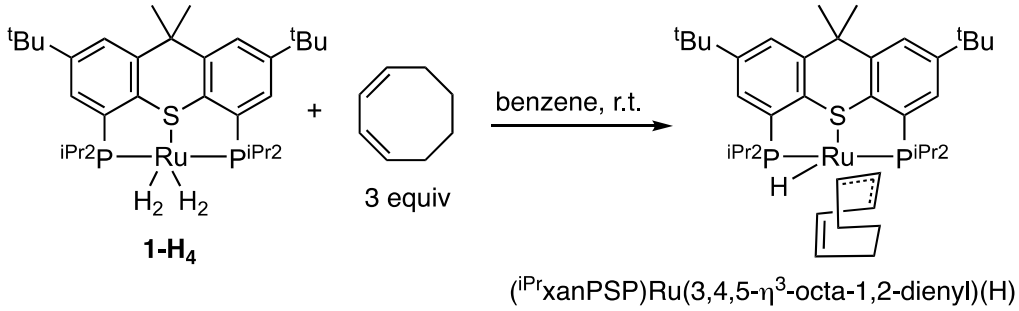

Scheme 5. Reaction of 1,3-Cyclooctadiene with (^{iPr}xanPSP)Ru(H$_2$)$_2$ (1-H$_4$)

4. DFT Calculations. Electronic structure calculations based on density functional theory (DFT) support and allow us to expand upon our interpretations, presented above, of the catalytic activity of (^{iPr}xanPSP)Ru complexes, particularly as compared with analogous (^{iPr}PCP)Ir complexes. DFT calculations were carried out on the reactions discussed above using the M06 functional. We replaced the inner electrons in metal atoms by effective core potentials and applied valence basis sets of triple-zeta quality or better for all atoms.[64]

4.1. Dehydrogenation of n-*Alkanes.* The (^{iPr}xanPSP)Ru fragment itself was calculated to be extremely reactive for alkane dehydrogenation, much more so than the (^{iPr}PCP)Ir analogue.

For 1,2-dehydrogenation of *n*-hexane the free energies of the transition states (TSs) for *n*-hexane C-H addition to (^{iPr}xanPSP)Ru (**TS$_{2\text{-}3}$**) and subsequent β-H elimination (**TS$_{3\text{-}4}$**) were calculated to be, respectively, 0.7 kcal/mol and 9.4 kcal/mol *below* that of the free three-coordinate fragment plus *n*-hexane (7.6 M) (Figure 6a). The TS for C-H addition (**TS$_{2\text{-}3}$**) connects a σ-C-H bond complex, **2** (ΔG = -9.4 kcal/mol) with the *n*-alkyl hydride, **3** (ΔG = -8.7 kcal/mol) (all free energies are expressed relative to the free (pincer)metal fragment and appropriate organic molecules unless specified otherwise). The TS for β-H elimination (**TS$_{3\text{-}4}$**) leads to a 1-hexene *cis*-dihydride complex (**4**) with ΔG = -20.2 kcal/mol; note that **TS$_{3\text{-}4}$**, although of course higher on the electronic energy surface (by only 0.4 kcal/mol) is actually calculated to be lower in free energy than the alkyl hydride complex **3**. Attempts to find a TS for loss of 1-hexene led instead to a transition state (**TS$_{4\text{-}5}$**) which connected to a complex (**5**) in which a 1-hexene C(4)-H bond is bound in a sigma fashion to the Ru center ($d_{Ru\text{-}H}$ = 2.14 Å)[81] with ΔG = -4.7 kcal/mol. The structure of the (PSP)RuH_2 unit is very nearly the same in both this σ-C-H complex and the unbound (^{iPr}xanPSP)RuH_2 product. While a TS for dissociation of 1-hexene from this complex could not be located, we can therefore presume that the enthalpic barrier in the reverse direction (σ-C-H bond coordination to (^{iPr}xanPSP)RuH_2) is very small, and the enthalpic barrier

for loss of 1-hexene is therefore approximately equal to that of the enthalpy of binding (13.0 kcal/mol). If we assume that $\Delta S^{\ddagger}$ for this dissociative process is ca. 10-20 eu, then (at 298 K) $\Delta G^{\ddagger}$ for this step is 7 - 10 kcal/mol, and the energy of the hypothetical transition state for loss of 1-hexene is inferred to be between ΔG = 2.3 kcal/mol and ΔG = 5.3 kcal/mol. As approached from the reverse direction, the free energy of this TS may be estimated by again assuming that coordination of the C-H bond to (^{iPr}xanPSP)RuH_2 has no significant enthalpic barrier, and therefore the rate is nearly diffusion limited. Assuming a rate constant between 10^7 $M^{-1}\cdot s^{-1}$ and 10^9 $M^{-1}\cdot s^{-1}$ implies a barrier for coordination, $\Delta G^{\ddagger}_{298}$, between 5.2 and 7.9 kcal/mol, which corresponds to a TS with free energy between 2.6 kcal/mol and 5.3 kcal/mol, consistent with the above estimate. (For the sake of clarity we express this estimated free energy of the hypothetical transition state as 4 ± 2 kcal/mol in Figure 6).

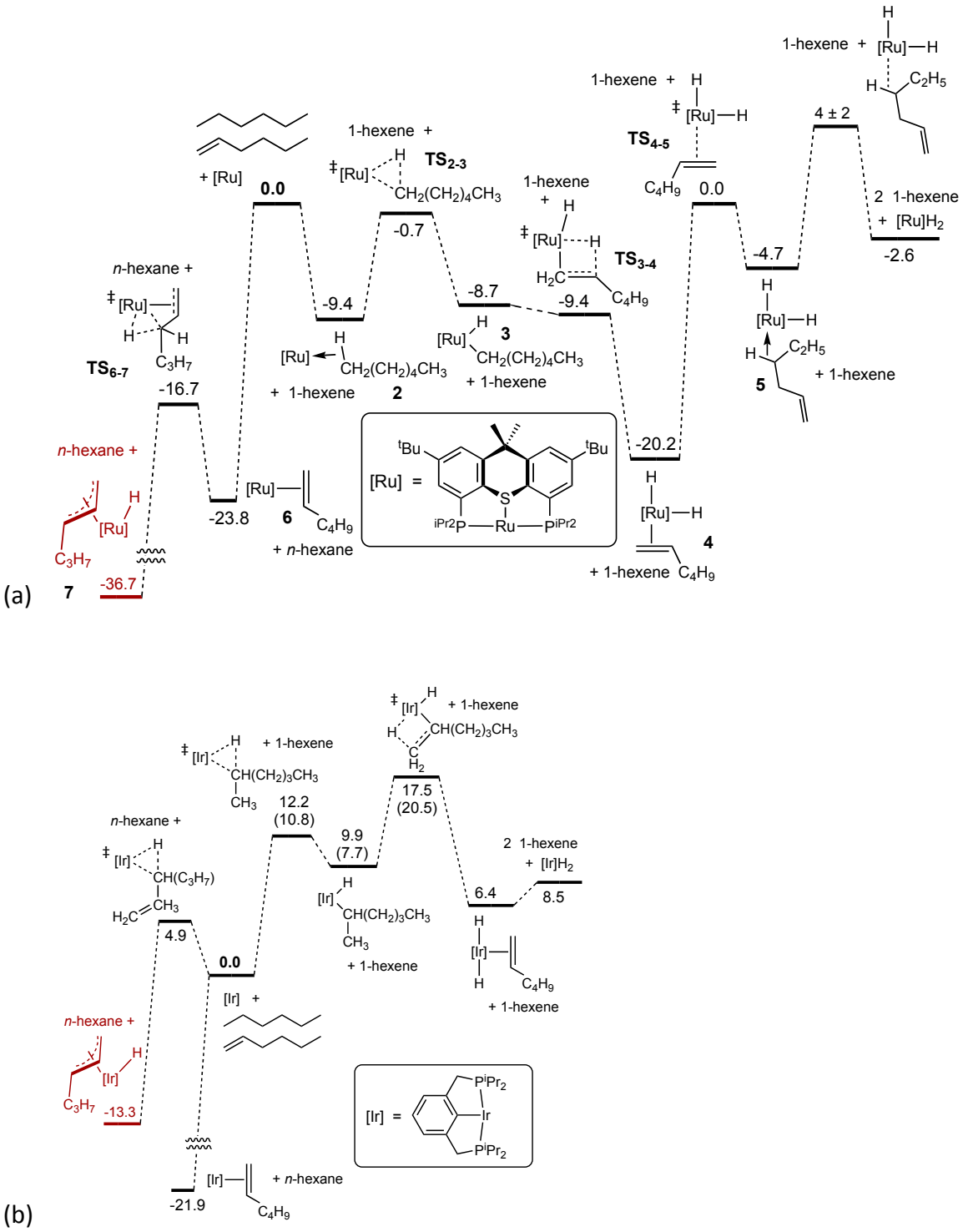

Figure 6. Free energy profile (kcal/mol) of 1,2-dehydrogenation of *n*-hexane by (a) (^{iPr}xanPSP)Ru and (b) (^{iPr}PCP)Ir. Free energies calculated for [*n*-hexane] = 7.65 M (concentration of neat solvent) and for [1-hexene] = 1.0 M. "‡" indicates calculated transition state.

Based on the above considerations, and as illustrated in Figure 6a, loss of 1-hexene from (^{iPr}xanPSP)RuH_2(1-hexene) (**4**), proceeding via **5**, is the calculated rate-determining step for *n*-hexane dehydrogenation by (^{iPr}xanPSP)Ru. If the resting state were (^{iPr}xanPSP)Ru(1-hexene) (**6**) (ΔG = -23.8 kcal/mol), the overall barrier to dehydrogenation would be [(4 ± 2) - (-23.8)] kcal/mol or 28 ± 2 kcal/mol, corresponding to a fairly rapid reaction (e.g. ca. 0.03 s^{-1} at 150 °C). (For a transfer-dehydrogenation cycle, subsequent hydrogenation of an acceptor like 1-hexene, i.e. the reverse reaction, has a much lower barrier.) However, (^{iPr}xanPSP)Ru(1-hexene) is calculated to undergo facile tautomerization via **$TS_{6\text{-}7}$** ($\Delta G^{\ddagger}$ = 7.1 kcal/mol) to give (^{iPr}xanPSP)Ru(η^3-hexen-3-yl)(H) (**7**), which is 12.9 kcal/mol lower in free energy than **6**. Thus the calculated overall barrier for dehydrogenation is ca. 41 ± 2 kcal/mol, consistent with the very slow observed rates and of course consistent with the observation of an allyl hydride resting state.[82]

Note that the very unsymmetric bowl-like structure of the (^{iPr}xanPSP)Ru unit results in two possible diastereomers for the complexes shown in Figure 6a. The lower-energy diastereomers (free energies shown) are those in which the bulkier substituents are located "outside the bowl" (exo vs. endo). For example the endo product of 1-hexyl C-H addition and the corresponding TS are, respectively, 3.6 kcal/mol and 3.5 kcal/mol higher than the exo isomers. The difference is much greater for the more crowded product of β-H elimination (**4**) and the corresponding transition state (**$TS_{3\text{-}4}$**); the endo analogues are 16.3 kcal/mol and 16.0 kcal/mol higher in free energy, respectively. This large effect of pincer ligand conformation may have significant implications for future catalyst design.

In contrast with (^{iPr}xanPSP)Ru, 1,2-dehydrogenation of *n*-hexane by the (^{iPr}PCP)Ir fragment is calculated to have significant barriers to C-H addition and β-H-elimination: ΔG = 12.2 kcal/mol

and 17.5 kcal/mol, respectively (Figure 6b). (These values are for a pathway proceeding via initial addition of the C(2)-H bond; for a pathway proceeding via initial addition of the C(1)-H bond, the respective values are 10.8 kcal/mol and 20.5 kcal/mol). Since these barriers are much higher than those in the reaction of (^{iPr}xanPSP)Ru, while the free energy of the binding of 1-hexene to (^{iPr}PCP)Ir is comparable to that of 1-hexene binding to (^{iPr}xanPSP)Ru, the Ru fragment would be much more reactive than (^{iPr}PCP)Ir if the respective η^2-1-hexene complex were the resting state in both cases. However, in contrast with (^{iPr}xanPSP)Ru, for (^{iPr}PCP)Ir the corresponding allyl hydride, although accessible as an intermediate out-of-cycle species,[69, 83] is *higher* in free energy than the olefin complex and therefore does not result in catalyst inhibition. The magnitude of the difference in the relative energies of these species is striking; isomerization of the η^2-1-hexene complex to the η^3-allyl hydride is endergonic by 8.6 kcal/mol for (^{iPr}PCP)Ir, vs. 12.9 kcal/mol exergonic for (^{iPr}xanPSP)Ru; thus $\Delta\Delta G$ = 21.5 kcal/mol.

4.2. Dehydrogenation of Cyclooctane. The η^2-cyclooctene complex of (^{iPr}xanPSP)Ru is calculated to have a free energy that is 16.4 kcal/mol below that of the free species (Figure 7a). This represents substantially weaker binding than to 1-hexene (23.8 kcal/mol). An even greater difference between the COE and 1-alkene complexes concerns tautomerization to give the allyl hydride which, as noted above, is 12.9 kcal/mol exergonic for 1-hexene; by contrast, the η^3-cyclooctenyl hydride complex of (^{iPr}xanPSP)Ru is calculated to be slightly higher in free energy (by 1.3 kcal/mol) than the η^2-cyclooctene complex (Figure 7). The 3,4,5-η^3-octa-1,2-dienyl complex, however, is calculated to have a free energy that is surprisingly lower than the η^3-cyclooctenyl complex (ΔG = -23.7 kcal/mol vs. -15.1 kcal/mol).

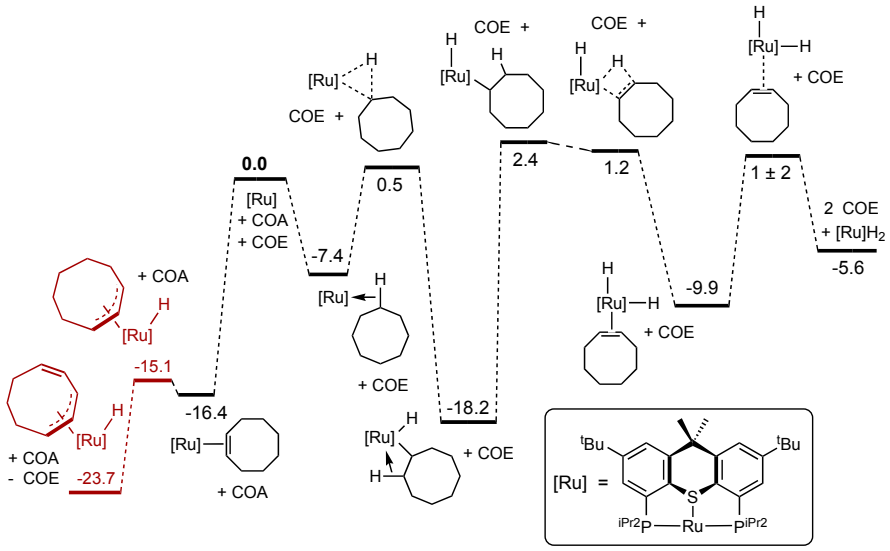

(a)

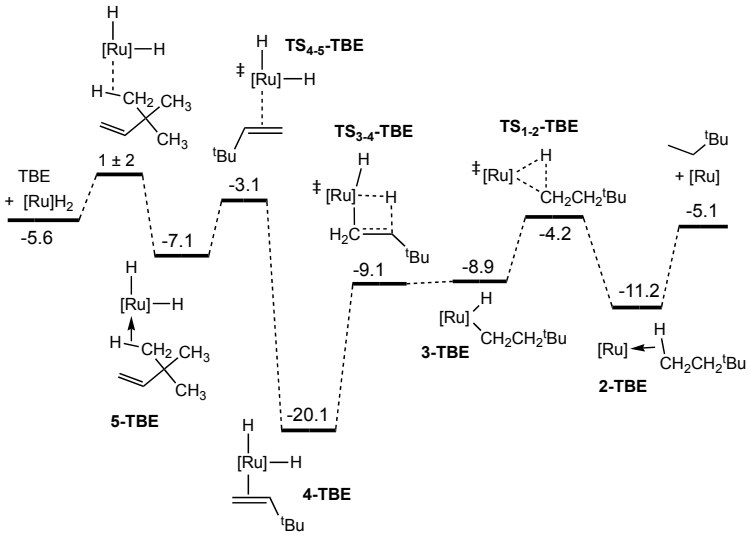

(b)

Figure 7. Free energy profile (kcal/mol) of (a) dehydrogenation of COA and (b) hydrogenation of TBE, by (^{iPr}xanPSP)Ru. Free energies calculated for [COA] = 7.43 M (concentration of neat solvent) and for [COE] = [TBE] = 1.0 M. "‡" indicates calculated transition state. Energies of TBE reaction profile are relative to that of (^{iPr}xanPSP)RuH_2 plus TBE, which is set at -5.6 kcal/mol to facilitate combination of COA dehydrogenation and TBE hydrogenation. (See Figure S45 for corresponding profile for COA dehydrogenation by (^{iPr}PCP)Ir.)

C-H addition of COA, as with *n*-hexane, is calculated to be very facile, with a TS that is only 0.5 kcal/mol higher in free energy than the free species (Figure 7a). This TS connects to an alkyl hydride which has a pronounced β-H agostic interaction (d_{Ru-H} = 1.915 Å) and a low free energy

(ΔG = -18.2 kcal/mol). (We have previously shown that the cyclooctyl group can form a particularly strong agostic bond since the eclipsed C-H bond interactions that are required for agostic bond formation are already present in the non-agostic cyclooctyl group, as well as in the free alkane, being responsible for the well known ring strain of COA.[7]) β-H elimination directly from the agostic species would lead to the trans-dihydride COE complex, but in fact, the lowest calculated β-H elimination leads to the cis-dihydride COE complex; therefore loss of the agostic interaction must precede β-H elimination. The resulting cyclooctyl ruthenium hydride, as was found for 1-hexyl hydride, is slightly higher in free energy (ΔG = 2.4 kcal/mol) than the β-H elimination TS (ΔG = 1.2 kcal/mol). The overall barrier for the dehydrogenation (Figure 7a) from a 3,4,5-η^3-octa-1,2-dienyl resting state is calculated to be 26.1 kcal/mol under the assumed concentrations of 7.4 M COA and 1.0 M COE. Under typical reaction conditions, with [COE] increasing from 0 to 0.3 M, the free energy barrier would be lower; e.g. at 0.1 M COE it would be lower by TΔS = T(2 x R·ln10) = 2.7 kcal/mol (two mol COE are liberated in the pathway from η^3-octa-1,2-dienyl resting state to the β-H elimination TS) to give a total $\Delta G^{\ddagger}$ = 23.4 kcal/mol.

The subsequent reaction of (^{iPr}xanPSP)RuH_2 with TBE to regenerate the reactive fragment (^{iPr}xanPSP)Ru is calculated to be very fast (Figure 7b). As with 1-hexene, attempts to locate the TS for the addition of TBE to (^{iPr}xanPSP)RuH_2 to yield (^{iPr}xanPSP)RuH_2(π-olefin) only led to a TS (**TS$_{4\text{-}5}$-TBE**) connecting the π-olefin dihydride complex (**4-TBE**) with a σ-C(4)-H complex (i.e. a *t*-butyl σ-C-H complex, **5-TBE**). The free energy of this TS is only 2.5 kcal/mol above free TBE and (^{iPr}xanPSP)RuH_2. Formation of the sigma complex from the free species appears to have no barrier on the energy surface; a diffusion-controlled rate, with an effective barrier of $\Delta G^{\ddagger}$ between ca. 5 and 8 kcal/mol as discussed above, would therefore be rate-limiting for formation

of (^{iPr}xanPSP)RuH_2(π-TBE) (**4-TBE**). **4-TBE** is more crowded than the analogous 1-hexene complex and its free energy is only 14.5 kcal/mol below that of free olefin plus (^{iPr}xanPSP)RuH_2 (cf. 17.6 kcal/mol for 1-hexene). Subsequent insertion of the TBE double-bond into an Ru-H bond is kinetically facile; the transition state (**$TS_{3\text{-}4}$-TBE**) is lower in free energy than that of the resulting alkyl hydride (**3-TBE**) as was found for the reaction of the analogous 1-hexene complex. The rate-determining step for the overall TBE hydrogenation is C-H reductive elimination of 2,2-dimethylbutane, the TS for which (**$TS_{1\text{-}2}$-TBE**) has a free energy only 15.9 kcal/mol above (PSP)RuH_2(π-TBE). The TBE hydrogenation component of the COA/TBE transfer dehydrogenation cycle is therefore even faster than the COA dehydrogenation. The free energy of activation for the COA dehydrogenation segment, $\Delta G^{\ddagger}$ = 23.4 kcal/mol, is therefore the activation free energy for the overall COA/TBE transfer dehydrogenation. This value compares quite well with a value of $\Delta G^{\ddagger} \cong$ 24.5 kcal/mol inferred from the rate of approximately 0.2 s^{-1} determined experimentally at 120 °C.

The same set of calculations that explains the rapid transfer-dehydrogenation of COA by (^{iPr}xanPSP)Ru also sheds light on its poor performance as a catalyst for acceptorless COA dehydrogenation, particularly as compared with (^{iPr}PCP)Ir (as described above). Although the TSs for loss of H_2 from neither (^{iPr}xanPSP)RuH_2 nor (^{iPr}PCP)IrH_2 could be located, the free energy of H_2 loss from the Ru complex is ΔG_{298} = 25.3 kcal/mol; this value is 11.1 kcal/mol greater than that for the much more effective acceptorless COA dehydrogenation catalyst, (^{iPr}PCP)IrH_2.

4.3. Stability of the Ruthenium Allyl Hydrides. The formation of stable linear allyl complexes, in contrast with the strained and crowded cyclic allyl complex, appears to be the key factor preventing (^{iPr}xanPSP)Ru from being a highly effective catalyst for dehydrogenation of linear

alkanes. This leads to the question as to why the isomerization of (^{iPr}xanPSP)Ru(η^2-1-hexene) to the η^3-hex-1-enyl complex is so much more favorable ($\Delta\Delta G$ = 21.5 kcal/mol) than the analogous reactions of (^{iPr}PCP)Ir complexes.

It is tempting to attribute the much greater tendency of (^{iPr}xanPSP)Ru^0(η^2-olefin) to undergo allylic C-H oxidative addition to give the Ru^{II} η^3-allyl hydride, as compared with the analogous Ir^I/Ir^{III} reaction, to the lower oxidation state of the Ru complex. The full explanation, however, is perhaps not quite so simple. For example, H_2 addition to the 14e fragments is "only" 11.1 kcal/mol more favorable for Ru^0 than for Ir^I. For H_2 addition to the corresponding 1-hexene complexes however, $\Delta\Delta G$ = 26.6 kcal/mol favoring Ru^0, an amount even greater than the 21.5 kcal/mol for the η^2-olefin to η^3-allyl hydride interconversion. This is consistent with results of previous studies in our lab in which it was found that H-H or C-H "oxidative" addition to three-coordinate d^8 (pincer)M fragments is not physically oxidative,[10, 84] whereas addition of the same substrates to four-coordinate d^8 complexes such as (pincer)M(olefin) and (pincer)M(CO) do in fact have a significant oxidative component;[10] those additions are therefore significantly more favorable for the more electron-rich species. We propose that this largely accounts for the high stability of the Ru^{II} η^3-allyl hydrides, although more detailed investigation of the characteristics of (^{iPr}xanPSP)M fragments are currently underway in our laboratory.

■ CONCLUSIONS

We report the development of a (PSP)Ru system for the transfer dehydrogenation of alkanes. For the "benchmark" COA/TBE transfer dehydrogenation, average TOFs are measured to be on the order of 1 s^{-1} at 180 °C. Since the reaction approaches completion within 5 min

(approximately the time required to reach that temperature), TOFs are presumably much higher at certain time points. Even at 120 °C, an average TOF as high as 0.2 s^{-1} is obtained. Rates and turnover numbers with linear alkanes, however, are much lower. Linear allyl complexes (PSP)Ru(η^3-alkenyl)(H) have been observed and isolated, during and after catalysis with *n*-alkanes.

The DFT calculations afford insight into the high but limited activity of the (^{iPr}xanPSP)Ru system. Compared with the closely related catalytically active fragment, (^{iPr}PCP)Ir, calculated free energies of the respective in-cycle species and η^2-alk-1-ene complexes would suggest that the (^{iPr}xanPSP)Ru system would be significantly more active. However, in the case of linear olefins, the corresponding η^3-allyl hydride complexes are calculated to be extremely stable, in accord with experimental observations, and this stability is responsible for the low activity of the (^{iPr}xanPSP)Ru with *n*-alkanes.

Consideration of catalysts for alkane functionalization and dehydrogenation in particular often focuses on the C-H activation step or perhaps the subsequent β-H elimination step. But the free energy of the resting state, as in any catalytic cycle, is equally important. This work highlights that variations in the nature and energy of the resting state may be even more important than the variability in free energy of either the C-H activation or β-H elimination step. In the case of *n*-alkane dehydrogenation, the very great difference between the stability of η^3-linear-allyl hydride complexes of (^{iPr}PCP)Ir vs. (^{iPr}xanPSP)Ru explains the much greater effectiveness of the former, while the relative instability of η^3-cyclooctenyl complexes allows (^{iPr}xanPSP)Ru to be much more active than (^{iPr}PCP)Ir for dehydrogenation of cyclooctane. Alkane dehydrogenation catalyzed by complexes of the type considered in this work requires that the metal center undergoes C-H

addition and then β-H elimination; the valence-electron count of the active fragment must therefore also permit the formation of the corresponding allyl hydride complexes. Perhaps of particular note in this context, (PCP)Ru-based alkane dehydrogenation catalysts have proven to be the most effective alternatives to (PCP)Ir, and certainly the most effective Ru-based species.[16, 44] Because the valence electron count of the (PCP)Ru fragment is 15e (cf. 14e for (PSP)Ru or (PCP)Ir), the corresponding olefin complexes (e.g. (PCP)Ru(olefin)H) cannot undergo tautomerism to give a higher-oxidation-state allyl complex. To our knowledge, the stability of η^3-allyl complexes has never previously been proposed as a major factor determining the activity of alkane dehydrogenation catalysts; this work indicates, however, that it should be an important consideration in the design of such catalysts.

■ AUTHOR INFORMATION

Corresponding Author

E-mail: alan.goldman@rutgers.edu

ORCID Alan S. Goldman: 0000-0002-2774-710X

Notes

The authors declare no competing financial interest. Crystallographic data for compounds **1-(C_2H_4)$_2$** and **1-(η^3-allyl)(H)** are also deposited as CCDC 1885250 and 1885251.

■ ASSOCIATED CONTENT

Supporting Information. The Supporting Information is available free of charge on the ACS Publications website at DOI: xxxxx. : Detailed experimental and synthetic procedures, NMR data, computational details and reaction free energy diagrams, optimized structures for computational species (.mol format), and crystallographic details CCDC 1885250 and 1885251.

■ **ACKNOWLEDGEMENTS**

We thank the National Science Foundation for support of this work through Grant CHE-1465203, and through the CCI Center for Enabling New Technologies through Catalysis (CENTC) Phase II Renewal (CHE-1205189).

■ **REFERENCES**

(1) Brandts, J. A. M.; Kruiswijk, E.; Boersma, J.; Spek, A. L.; van Koten, G., C-H Activation of an MeN Grouping in one of the CH_2NMe_2 ortho Substituents of an NCN 'pincer' ligand in Tungsten Chemistry: X-ray Structure of [WCl_2(NPh)(C_6H_3{CH_2NMeCH_2}-2-{CH_2NMe_2}-6)] *J. Organomet. Chem.* **1999,** *585*, 93-99.
(2) Hollas, A. M.; Gu, W.; Bhuvanesh, N.; Ozerov, O. V., Synthesis and Characterization of Pd Complexes of a Carbazolyl/Bis(Imine) NNN Pincer Ligand *Inorg. Chem.* **2011,** *50*, 3673-3679.
(3) Jia, X.; Huang, Z., Conversion of Alkanes to Linear Alkylsilanes using an Iridium-Iron-Catalyzed Tandem Dehydrogenation-Isomerization-Hydrosilylation *Nature Chem.* **2016,** *8*, 157-161.
(4) Maji, M.; Chakrabarti, K.; Paul, B.; Roy, B. C.; Kundu, S., Ruthenium(II)-NNN-Pincer-Complex-Catalyzed Reactions Between Various Alcohols and Amines for Sustainable C-N and C-C Bond Formation *Adv. Synth. Catal.* **2018,** *360*, 722-729.
(5) Zell, T.; Milstein, D., Hydrogenation and Dehydrogenation Iron Pincer Catalysts Capable of Metal-Ligand Cooperation by Aromatization/Dearomatization *Acc. Chem. Res.* **2015,** *48*, 1979-1994.
(6) Bonitatibus, P. J., Jr.; Chakraborty, S.; Doherty, M. D.; Siclovan, O.; Jones, W. D.; Soloveichik, G. L., Reversible Catalytic Dehydrogenation of Alcohols for Energy Storage *Proc. Natl. Acad. Sci. U. S. A.* **2015,** *112*, 1687-1692.
(7) Bezier, D.; Guan, C.; Krogh-Jespersen, K.; Goldman, A. S.; Brookhart, M., Experimental and Computational Study of Alkane Dehydrogenation Catalyzed by a Carbazolide-based Rhodium PNP Pincer Complex *Chem. Sci.* **2016,** *7*, 2579-2586.
(8) Obligacion, J. V.; Bezdek, M. J.; Chirik, P. J., C(sp^2)-H Borylation of Fluorinated Arenes using an Air-stable Cobalt Precatalyst: Electronically Enhanced Site Selectivity Enables Synthetic Opportunities *J. Am. Chem. Soc.* **2017,** *139*, 2825-2832.
(9) Zeng, R.; Feller, M.; Ben-David, Y.; Milstein, D., Hydrogenation and Hydrosilylation of Nitrous Oxide Homogeneously Catalyzed by a Metal Complex *J. Am. Chem. Soc.* **2017,** *139*, 5720-5723.
(10) Lease, N.; Pelczar, E. M.; Zhou, T.; Malakar, S.; Emge, T. J.; Hasanayn, F.; Krogh-Jespersen, K.; Goldman, A. S., PNP-Pincer Complexes of Osmium: Comparison with Isoelectronic (PCP)Ir and (PNP)Ir^+ Units *Organometallics* **2018,** *37*, 314-326.
(11) Hermann, D.; Gandelman, M.; Rozenberg, H.; Shimon, L. J. W.; Milstein, D., Synthesis, Structure, and Reactivity of New Rhodium and Iridium Complexes, Bearing a Highly Electron-Donating PNP System. Iridium-Mediated Vinylic C-H Bond Activation *Organometallics* **2002,** *21*, 812-818.

(12) Bergbreiter, D. E.; Osburn, P. L.; Liu, Y.-S., Tridentate SCS Palladium(II) Complexes: New, Highly Stable, Recyclable Catalysts for the Heck Reaction *J. Am. Chem. Soc.* **1999,** *121*, 9531-9538.
(13) Yu, K.; Sommer, W.; Richardson, J. M.; Weck, M.; Jones, C. W., Evidence that SCS Pincer Pd(II) Complexes are only Precatalysts in Heck Catalysis and the Implications for Catalyst Recovery and Reuse *Adv. Synth. Catal.* **2005,** *347*, 161-171.
(14) Schörgenhumer, J.; Zimmermann, A.; Waser, M., SNS-Ligands for Ru-Catalyzed Homogeneous Hydrogenation and Dehydrogenation Reactions *Org. Process Res. Dev.* **2018,** *22*, 862-870.
(15) Serra, D.; Cao, P.; Cabrera, J.; Padilla, R.; Rominger, F.; Limbach, M., Development of Platinum(II) and -(IV) CNC Pincer Complexes and Their Application in a Hydrovinylation Reaction *Organometallics* **2011,** *30*, 1885-1895.
(16) Gruver, B. C.; Adams, J. J.; Warner, S. J.; Arulsamy, N.; Roddick, D. M., Acceptor Pincer Chemistry of Ruthenium: Catalytic Alkane Dehydrogenation by (CF_3PCP)Ru(cod)(H) *Organometallics* **2011,** *30*, 5133–5140.
(17) Musa, S.; Ackermann, L.; Gelman, D., Dehydrogenative Cross-Coupling of Primary and Secondary Alcohols *Adv. Synth. Catal.* **2013,** *355*, 3077-3080.
(18) Timpa, S. D.; Pell, C. J.; Ozerov, O. V., A Well-Defined (POCOP)Rh Catalyst for the Coupling of Aryl Halides with Thiols *J. Am. Chem. Soc.* **2014,** *136*, 14772-14779.
(19) Murugesan, S.; Kirchner, K., Non-precious Metal Complexes with an Anionic PCP Pincer Architecture *Dalton Trans.* **2016,** *45*, 416-439.
(20) Albrecht, M.; van Koten, G., Platinum Group Organometallics Based on "Pincer" Complexes: Sensors, Switches, and Catalysts. *Angew. Chem., Intl. Ed.* **2001,** *40*, 3750-3781.
(21) *The Chemistry of Pincer Compounds;* Morales-Morales, D.; Jensen, C., Eds.; Elsevier: Amsterdam, 2007.
(22) Musa, S.; Shaposhnikov, I.; Cohen, S.; Gelman, D., Ligand-Metal Cooperation in PCP Pincer Complexes: Rational Design and Catalytic Activity in Acceptorless Dehydrogenation of Alcohols *Angew. Chem., Intl. Ed.* **2011,** *50*, 3533-3537.
(23) Selander, N.; Szabo, K. J., Catalysis by Palladium Pincer Complexes *Chem. Rev.* **2011,** *111*, 2048-2076.
(24) Salah, A. B.; Offenstein, C.; Zargarian, D., Hydroamination and Alcoholysis of Acrylonitrile Promoted by the Pincer Complex {κP,κC,κP-2,6-$(Ph_2PO)_2C_6H_3$}Ni(OSO_2CF_3) *Organometallics* **2011,** *30*, 5352-5364.
(25) Albrecht, M.; Lindner, M. M., Cleavage of Unreactive Bonds with Pincer Metal Complexes *Dalton Trans.* **2011,** *40*, 8733-8744.
(26) Helgert, T. R.; Hollis, T. K.; Valente, E. J., Synthesis of Titanium CCC-NHC Pincer Complexes and Catalytic Hydroamination of Unactivated Alkenes *Organometallics* **2012,** *31*, 3002-3009.
(27) Gelman, D.; Musa, S., Coordination Versatility of sp^3-Hybridized Pincer Ligands toward Ligand-Metal Cooperative Catalysis *ACS Catal.* **2012,** *2*, 2456-2466.
(28) Kang, P.; Cheng, C.; Chen, Z.; Schauer, C. K.; Meyer, T. J.; Brookhart, M., Selective Electrocatalytic

Reduction of CO_2 to Formate by Water-Stable Iridium Dihydride Pincer Complexes *J. Am. Chem. Soc.* **2012,** *134*, 5500-5503.
(29) Szabo, K. J., Pincer Complexes as Catalysts in Organic Chemistry *Top. Organomet. Chem.* **2013,** *40*, 203-242.
(30) van Koten, G., Pincer Ligands as Powerful Tools for Catalysis in Organic Synthesis *J. Organomet. Chem.* **2013,** *730*, 156-164.
(31) van Koten, G., The Monoanionic ECE-Pincer Ligand: A Versatile Privileged Ligand Platform—General Considerations. In *Organometallic Pincer Chemistry*, van Koten, G.; Milstein, D., Eds. Springer Berlin Heidelberg: Berlin, Heidelberg, 2013; pp 1-20.
(32) Gutsulyak, D. V.; Piers, W. E.; Borau-Garcia, J.; Parvez, M., Activation of Water, Ammonia, and Other Small Molecules by $PC_{carbene}P$ Nickel Pincer Complexes *J. Am. Chem. Soc.* **2013,** *135*, 11776-11779.
(33) Hao, J.; Mougang-Soume, B.; Vabre, B.; Zargarian, D., On the Stability of a $POC_{sp3}OP$-Type Pincer Ligand in Nickel(II) Complexes *Angew. Chem., Intl. Ed.* **2014,** *53*, 3218-3222.
(34) Chakraborty, S.; Bhattacharya, P.; Dai, H.; Guan, H., Nickel and Iron Pincer Complexes as Catalysts for the Reduction of Carbonyl Compounds *Acc. Chem. Res.* **2015,** *48*, 1995-2003.
(35) Hanninen, M. M.; Zamora, M. T.; Hayes, P. G., Rare Earth Pincer Complexes: Synthesis, Reaction Chemistry, and Catalysis *Top. Organomet. Chem.* **2016,** *54*, 93-177.
(36) Crabtree, R. H., Homogeneous Transition Metal Catalysis of Acceptorless Dehydrogenative Alcohol Oxidation: Applications in Hydrogen Storage and to Heterocycle Synthesis *Chem. Rev.* **2017,** *117*, 9228-9246.
(37) Mukherjee, A.; Srimani, D.; Ben-David, Y.; Milstein, D., Low-Pressure Hydrogenation of Nitriles to Primary Amines Catalyzed by Ruthenium Pincer Complexes. Scope and mechanism *ChemCatChem* **2017,** *9*, 559-563.
(38) Valdes, H.; Garcia-Eleno, M. A.; Canseco-Gonzalez, D.; Morales-Morales, D., Recent Advances in Catalysis with Transition-Metal Pincer Compounds *ChemCatChem* **2018,** *10*, 3136-3172.
(39) Kumar, A.; Goldman, A. S., Recent Advances in Alkane Dehydrogenation Catalyzed by Pincer Complexes. In *The Privileged Pincer-Metal Platform: Coordination Chemistry & Applications*, van Koten, G.; Gossage, R. A., Eds. Springer International Publishing: Cham, 2016; pp 307-334.
(40) Kumar, A.; Bhatti, T. M.; Goldman, A. S., Dehydrogenation of Alkanes and Aliphatic Groups by Pincer-Ligated Metal Complexes *Chem. Rev.* **2017,** *117*, 12357-12384.
(41) Haibach, M. C.; Wang, D. Y.; Emge, T. J.; Krogh-Jespersen, K.; Goldman, A. S., (POP)Rh Pincer Hydride Complexes: Unusual Reactivity and Selectivity in Oxidative Addition and Olefin Insertion Reactions *Chem. Sci.* **2013,** *4*, 3683-3692.
(42) Allen, K. E.; Heinekey, D. M.; Goldman, A. S.; Goldberg, K. I., Alkane Dehydrogenation by C-H Activation at Iridium(III) *Organometallics* **2013,** *32*, 1579-1582.
(43) Cheng, C.; Kim, B. G.; Guironnet, D.; Brookhart, M.; Guan, C.; Wang, D. Y.; Krogh-Jespersen, K.; Goldman, A. S., Synthesis and Characterization of Carbazolide-based Iridium PNP Pincer Complexes.

Mechanistic and Computational Investigation of Alkene Hydrogenation: Evidence for an Ir(III)/Ir(V)/Ir(III) Catalytic Cycle *J. Am. Chem. Soc.* **2014,** *136*, 6672−6683.
(44) Zhang, Y.; Fang, H.; Yao, W.; Leng, X.; Huang, Z., Synthesis of Pincer Hydrido Ruthenium Olefin Complexes for Catalytic Alkane Dehydrogenation *Organometallics* **2016,** *35*, 181-188.
(45) Gunanathan, C.; Milstein, D., Bond Activation and Catalysis by Ruthenium Pincer Complexes *Chem. Rev.* **2014,** *114*, 12024−12087.
(46) Balaraman, E.; Milstein, D., Hydrogenation of Polar Bonds Catalysed by Ruthenium-Pincer Complexes *Top. Organomet. Chem.* **2015,** *48*, 19-43.
(47) Murray, S. G.; Hartley, F. R., Coordination Chemistry of Thioethers, Selenoethers, and Telluroethers in Transition-Metal Complexes *Chem. Rev.* **1981,** *81*, 365-414.
(48) Masdeu-Bulto, A. M.; Dieguez, M.; Martin, E.; Gomez, M., Chiral Thioether Ligands: Coordination Chemistry and Asymmetric catalysis *Coord. Chem. Rev.* **2003,** *242*, 159-201.
(49) Esteruelas, M. A.; Honczek, N.; Olivan, M.; Onate, E.; Valencia, M., Direct Access to POP-type Osmium(II) and Osmium(IV) Complexes: Osmium a Promising Alternative to Ruthenium for the Synthesis of Imines from Alcohols and Amines *Organometallics* **2011,** *30*, 2468-2471.
(50) Adams, G. M.; Weller, A. S., POP-type Ligands: Variable Coordination and Hemilabile Behaviour *Coord. Chem. Rev.* **2018,** *355*, 150-172.
(51) Barbaro, P.; Bianchini, C.; Togni, A., Synthesis and Characterization of Ruthenium(II) Complexes Containing Chiral Bis(ferrocenyl)−P3 or −P2S Ligands. Asymmetric Transfer Hydrogenation of Acetophenone *Organometallics* **1997,** *16*, 3004-3014.
(52) Lee, H. M.; Bianchini, C.; Jia, G.; Barbaro, P., Styrene Cyclopropanation and Ethyl Diazoacetate Dimerization Catalyzed by Ruthenium Complexes Containing Chiral Tridentate Phosphine Ligands *Organometallics* **1999,** *18*, 1961-1966.
(53) Kuchison, A. M.; Wolf, M. O.; Patrick, B. O., Photophysical and Electrochemical Properties of Ru(II) Complexes Containing Tridentate Bisphosphino-Oligothiophene Ligands *Dalton Trans.* **2011,** *40*, 6912-6921.
(54) Sgro, M. J.; Stephan, D. W., Synthesis and Reactivity of Ruthenium Tridentate bis-Phosphinite Ligand Complexes *Dalton Trans.* **2013,** *42*, 10460-10472.
(55) Andreasen, L. V.; Simonsen, O.; Wernberg, O., Platinum(II) Complexes with the Tridentate Phosphino–Thioether Ligand Bis(2-diphenylphosphinoethyl)sulfide, $(PPh_2CH_2CH_2)_2S$. X-ray Crystal Structures of $[Pt\{(PPh_2CH_2CH_2)_2S\}Cl]ClO4$ and $[Pt\{(PPh_2CH_2CH_2)_2S\}I]I$ *Inorg. Chim. Acta.* **1999,** *295*, 153-163.
(56) Emslie, D. J. H.; Harrington, L. E.; Jenkins, H. A.; Robertson, C. M.; Britten, J. F., Group 10 Transition-Metal Complexes of an Ambiphilic PSB-Ligand: Investigations into η^3(BCC)-Triarylborane Coordination *Organometallics* **2008,** *27*, 5317-5325.
(57) Zuideveld, M. A.; Swennenhuis, B. H. G.; Boele, M. D. K.; Guari, Y.; van Strijdonck, G. P. F.; Reek, J. N. H.; Kamer, P. C. J.; Goubitz, K.; Fraanje, J.; Lutz, M.; Spek, A. L.; van Leeuwen, P. W. N. M., The Coordination Behaviour of Large Natural Bite Angle Diphosphine Ligands Towards Methyl and 4-

Cyanophenylpalladium(II) Complexes *J. Chem. Soc., Dalton Trans.* **2002**, 2308-2317.
(58) Morohashi, N.; Akahira, Y.; Tanaka, S.; Nishiyama, K.; Kajiwara, T.; Hattori, T., Synthesis of a Sulfur-bridged Diphosphine Ligand and Its Unique Complexation Properties toward Palladium(II) Ion *Chem. Lett.* **2008,** *37*, 418-419.
(59) Moxham, G. L.; Randell-Sly, H.; Brayshaw, S. K.; Weller, A. S.; Willis, M. C., Intermolecular Alkene and Alkyne Hydroacylation with β-S-Substituted Aldehydes: Mechanistic Insight into the Role of a Hemilabile P–O–P Ligand *Chem.-Eur. J.* **2008,** *14*, 8383-8397.
(60) Pike, S. D.; Pawley, R. J.; Chaplin, A. B.; Thompson, A. L.; Hooper, J. A.; Willis, M. C.; Weller, A. S., Exploring $(Ph_2PCH_2CH_2)_2E$ Ligand Space (E = O, S, PPh) in Rh(I) Alkene Complexes as Potential Hydroacylation Catalysts *Eur. J. Inorg. Chem.* **2011,** *2011*, 5558-5565.
(61) McGuinness, D. S.; Wasserscheid, P.; Morgan, D. H.; Dixon, J. T., Ethylene Trimerization with Mixed-Donor Ligand (N,P,S) Chromium Complexes: Effect of Ligand Structure on Activity and Selectivity *Organometallics* **2005,** *24*, 552-556.
(62) Tisato, F.; Refosco, F.; Porchia, M.; Bolzati, C.; Bandoli, G.; Dolmella, A.; Duatti, A.; Boschi, A.; Jung, C. M.; Pietzsch, H.-J.; Kraus, W., The Crucial Role of the Diphosphine Heteroatom X in the Stereochemistry and Stabilization of the Substitution-Inert $[M(N)(PXP)]^{2+}$ Metal Fragments (M = Tc, Re; PXP = Diphosphine Ligand) *Inorg. Chem.* **2004,** *43*, 8617-8625.
(63) Major, Q.; Lough, A. J.; Gusev, D. G., Substituents Effects in POP Pincer Complexes of Ruthenium *Organometallics* **2005,** *24*, 2492-2501.
(64) See Supporting Information for details.
(65) Asensio, G.; Cuenca, A. B.; Esteruelas, M. A.; Medio-Simon, M.; Olivan, M.; Valencia, M., Osmium(III) Complexes with POP Pincer Ligands: Preparation from Commercially Available $OsCl_3 \cdot 3H_2O$ and Their X-ray Structures *Inorg. Chem.* **2010,** *49*, 8665-8667.
(66) Alos, J.; Bolano, T.; Esteruelas, M. A.; Olivan, M.; Onate, E.; Valencia, M., POP-Pincer Osmium-Polyhydrides: Head-to-Head (Z)-Dimerization of Terminal Alkynes *Inorg. Chem.* **2013,** *52*, 6199-6213.
(67) Anton, D. R.; Crabtree, R. H., Mercury Test for Colloids *Organometallics* **1983,** *2*, 855-859.
(68) The fastest previously reported examples of transfer-dehydrogenation at their respective temperatures above 150 °C are, to our knowledge, the following. Our lab reported n-octane/propene transfer dehydrogenation at 160 °C by (^{iPr}PCP)Ir with 450 TO obtained after 40 min (average TOF = 0.19 s^{-1})(ref 69). At 180 °C, the same system afforded 340 TO after 5 min (average TOF = 1.1 s^{-1}). At 170 °C, Wendt and co-workers reported COA/TBE transfer dehydrogenation by [3,5-$(CF_3)_2$ ^{tBu4}POCOP]Ir, with 625 TO obtained in 10 min (average TOF = 1.04 s^{-1})(ref 70). At 200 °C, Brookhart and co-workers obtained 1162 TO in COA/TBE transfer dehydrogenation by [3,5-$(CF_3)_2C_6H_3$-^{tBu}POCOP]Ir within 8 min (average TOF = 2.42 s^{-1})(ref 71). At 240 °C, we found that solid (^{iPr}PCP)Ir effected gas-phase n-octane/ propene transfer dehydrogenation with 1930 TO obtained in 10 min (average TOF = 3.2 s^{-1})(ref 69).
(69) Kumar, A.; Zhou, T.; Emge, T. J.; Mironov, O.; Saxton, R. J.; Krogh-Jespersen, K.; Goldman, A. S., Dehydrogenation of *n*-Alkanes by Solid-Phase Molecular Pincer-Iridium Catalysts. High Yields of α-Olefin

Product *J. Am. Chem. Soc.* **2015,** *137*, 9894-9911.
(70) Kovalenko, O. O.; Wendt, O. F., An Electron Poor Iridium Pincer Complex for Catalytic Alkane Dehydrogenation *Dalton Trans.* **2016,** *45*, 15963-15969.
(71) GottkerSchnetmann, I.; White, P.; Brookhart, M., Iridium Bis(phosphinite) p-XPCP Pincer Complexes: Highly Active Catalysts for the Transfer Dehydrogenation of Alkanes *J. Am. Chem. Soc.* **2004,** *126*, 1804-1811.
(72) Jia, X.; Zhang, L.; Qin, C.; Leng, X.; Huang, Z., Iridium Complexes of New NCP Pincer Ligands: Catalytic Alkane Dehydrogenation and Alkene Isomerization *Chem. Commun.* **2014,** *50*, 11056-11059.
(73) Adams, J. J.; Arulsamy, N.; Roddick, D. M., Investigation of Iridium ^{CF3}PCP Pincer Catalytic Dehydrogenation and Decarbonylation Chemistry *Organometallics* **2012,** *31*, 1439-1447.
(74) Stull, D. R.; Westrum, E. F.; Sinke, G. C., *The Chemical Thermodynamics of Organic Compounds*. Robert E. Kreiger Publishing: Malabar, FL, 1987.
(75) All thermodynamic values obtained from: Afeefy, H. Y.; Liebman, J. F.; Stein, S.E. "Neutral Thermochemical Data" in NIST Chemistry WebBook, NIST Standard Reference Database Number 69, Eds. P.J. Linstrom and W.G. Mallard, National Institute of Standards and Technology, Gaithersburg MD, 20899, http://webbook.nist.gov, (retrieved September 24, 2018)
(76) Goldman, A. S.; Renkema, K. B.; Czerw, M.; Krogh-Jespersen, K., Alkane Transfer-Dehydrogenation Catalyzed by a Pincer-Ligated Iridium Complex. In *Activation and Functionalization of C-H Bonds*, Goldberg, K. I.; Goldman, A. S., Eds. Washington, DC, 2004; Vol. ACS Symposium Series 885, pp 198-215
(77) Liu, F.; Goldman, A. S., Efficient Thermochemical Alkane Dehydrogenation and Isomerization Catalyzed by an Iridium Pincer Complex *Chem. Commun.* **1999**, 655-656.
(78) Xue, P.; Bi, S.; Sung, H. H. Y.; Williams, I. D.; Lin, Z.; Jia, G., Isomerism of [Ru(η^3-allyl)Cl(CO)(PPh_3)$_2$] *Organometallics* **2004,** *23*, 4735-4743.
(79) Smart, K. A.; Grellier, M.; Vendier, L.; Mason, S. A.; Capelli, S. C.; Albinati, A.; Sabo-Etienne, S., Step-by-step Introduction of Silazane Moieties at Ruthenium: Different Extents of Ru-H-Si Bond Activation *Inorg. Chem.* **2013,** *52*, 2654-2661.
(80) Smart, K. A.; Grellier, M.; Coppel, Y.; Vendier, L.; Mason, S. A.; Capelli, S. C.; Albinati, A.; Montiel-Palma, V.; Munoz-Hernandez, M. A.; Sabo-Etienne, S., Nature of Si-H Interactions in a Series of Ruthenium Silazane Complexes Using Multinuclear Solid-State NMR and Neutron Diffraction *Inorg. Chem.* **2014,** *53*, 1156-1165.
(81) Brookhart, M.; Green, M. L. H.; Parkin, G., Agostic Interactions in Transition Metal Compounds *Proc. Natl. Acad. Sci.* **2007,** *104*, 6908-6914.
(82) Note that this barrier is calculated for 1 M 1-hexene and 7.6 M *n*-hexane. The rate would be inverse first order in 1-hexene and so, at a much lower concentration of free 1-hexene, the rate would be commensurately greater. Even at [1-hexene] = 1.0 mM, however, a free energy barrier of 41 kcal/mol ([1-hexene] = 1 M) corresponds to a rate of only 6 x10^{-6} s^{-1}.

(83) Biswas, S.; Huang, Z.; Choliy, Y.; Wang, D. Y.; Brookhart, M.; Krogh-Jespersen, K.; Goldman, A. S., Olefin Isomerization by Iridium Pincer Catalysts. Experimental Evidence for an eta-3-Allyl Pathway and an Unconventional Mechanism Predicted by DFT Calculations *J. Am. Chem. Soc.* **2012,** *134*, 13276-13295.

(84) Wang, D. Y.; Choliy, Y.; Haibach, M. C.; Hartwig, J. F.; Krogh-Jespersen, K.; Goldman, A. S., Assessment of the Electronic Factors Determining the Thermodynamics of “Oxidative Addition” of C–H and N–H Bonds to Ir(I) Complexes *J. Am. Chem. Soc.* **2016,** *138*, 149-163.

Table of Contents graphic for "Catalytic Alkane Transfer Dehydrogenation by PSP-pincer-ligated Ruthenium…"